GEOPHYSICAL RESEARCH LETTERS, VOL. 26, NO. 17, PAGES 2725-2728, SEPTEMBER 1, 1999

Comparison of Aerosol Optical Depth from Four Solar Radiometers During the Fall 1997 ARM Intensive Observation Period

B. Schmid,[1] J. Michalsky,[2] R. Halthore,[3] M. Beauharnois,[2] L. Harrison,[2]
J. Livingston,[4] P. Russell,[5] B. Holben,[6] T. Eck,[6,7] and A. Smirnov[6,8]

Abstract. In the Fall of 1997 the Atmospheric Radiation Measurement (ARM) program conducted an Intensive Observation Period (IOP) to study aerosols. Five sun-tracking radiometers were present to measure the total column aerosol optical depth. This comparison performed on the Southern Great Plains (SGP) demonstrates the capabilities and limitations of modern tracking sunphotometers at a location typical of where aerosol measurements are required. The key result was agreement in aerosol optical depth measured by 4 of the 5 instruments within 0.015 (rms). The key to this level of agreement was meticulous care in the calibrations of the instruments.

1. Introduction

In the last World Meteorological Organization workshop held to discuss the measurement of atmospheric optical depth [*WMO*, 1993] it was recommended that WMO's existing program to measure aerosol optical depth (AOD) within the Background Air Pollution Monitoring Network (BAPMoN) program, be discontinued and that the data that it had collected be regarded as suspect. The principal problem was that the instruments were unstable with regard to calibration, and the quality assurance provided no feedback to improve the quality of the observations.

New aerosol measurements under the auspices of the WMO were to be part of the Global Atmospheric Watch (GAW) program. Two of several specific recommendations for this new program in aerosol optical depth measurements were that automated sun-tracking would be required and that instruments to be used in the GAW program should be compared at a high altitude site.

In the Fall of 1997 the ARM program organized an IOP to study aerosol optical and physical properties using both remote sensing and in situ techniques. Five solar tracking radiometers for measuring total optical depth were present for the IOP leading to this *de facto* comparison along the guidelines of that recommended by the WMO. Although the comparison was not conducted at a high mountain site, there were several clear and stable days during the IOP.

The measurements were made between 15 September and 5 October 1997 at the SGP ARM central facility near Lamont, Oklahoma (36° 36' N, 97° 22' W, 316 m above sea level). Very low to moderate aerosol loading was experienced over the three-week period. Mid-visible AOD values ranged from 0.025 to 0.3. In all subsequent discussions, AOD is taken to mean the optical depth that is obtained by subtracting the Rayleigh component and any known gaseous component from the measured total optical depth.

2. Instrumentation

The NASA Ames Research Center deployed their six-channel Ames Airborne Tracking Sunphotometer (AATS-6) at the SGP central facility of ARM for this IOP. This instrument, described by *Matsumoto et al.* [1987], uses an active sun sensor to keep the instrument pointed at the solar disk. The central wavelengths and full widths at half maximum (FWHM) for the filters are given in Table 1. The Si detectors are held at a constant temperature of 45± 0.6 °C. The field-of-view (FOV) of AATS-6 is 4.5°. A measurement sequence was repeated every 12 seconds with all filters scanned nine times then averaged in the first three seconds of the 12-second period. The instrument was calibrated by averaging the results of 6 successful morning Langley plots [*Schmid et al.*, 1998] performed at the Mauna Loa Observatory in Hawaii (19° 32' N, 155° 34' W, 3397 m above sea level) about two weeks before the IOP.

At the ARM SGP central facility a CIMEL sun/sky photometer measures AOD. This instrument is also part of AERONET, a worldwide network of CIMEL sunphotometers [*Holben et al.*, 1998]. The CIMEL CE-318 points to the sun based on an ephemeris calculation and then fine tunes the pointing with an active sun sensor adjustment. Samples consist of triplets of measurements with each member of the triplet beginning 30 seconds apart and consisting of eight filter measurements completed within eight seconds; the triplets are repeated at every quarter air mass between two to five air masses and every 15 minutes when the air mass is less than two. The central wavelength and FWHM for each filter is given in Table 1. The field-of-view is 1.2°. The temperature of the instrument is monitored but not controlled. Calibration is based on a transfer of the calibration from an instrument that has recently been calibrated using the Langley technique at the Mauna Loa Observatory.

The multi-filter rotating shadowband radiometer (MFRSR) [*Harrison et al.*, 1994] has a hemispherical field-of-view. A band is positioned to alternately move completely out of the field-of-view and then to block the sun according to a solar

[1]Bay Area Environmental Research Institute, San Francisco, CA
[2]State University of New York, Albany, NY
[3]Brookhaven National Laboratory, Upton, NY
[4]SRI International, Menlo Park, CA
[5]NASA Ames Research Center, Moffett Field, CA
[6]NASA Goddard Space Flight Center, Greenbelt, MD
[7]Raytheon ITSS Corporation, Lanham, MD
[8]Science Systems and Applications Inc., Lanham, MD

Paper number 1999GL900513.
0094-8276/99/1999GL900513$05.00

Table 1. Central Wavelengths (λ) and Bandwidths ($\Delta\lambda$, Full Widths at Half Maximum) of Filtered Instruments.

AATS-6		CIMEL		MFRSR	
λ[nm]	$\Delta\lambda$ [nm]	λ [nm]	$\Delta\lambda$ [nm]	λ [nm]	$\Delta\lambda$ [nm]
		340	2		
380.1	5.0	380	4		
				413.9	10
450.7	5.1	440	10		
525.3	5.0	500	10	499.3	10
				608.5	10
		670	10	665.1	10
863.9	5.3	870	10	859.9	10
941.4	5.8	940	10	938.0	10
1020.7	5.0	1020	10		

hour angle calculation allowing a measurement of the total downward and diffuse downward irradiance. The difference between the two measurements is the direct solar component normal to the receiver, and the direct normal component is calculated by dividing by the cosine of the solar-zenith angle and correcting for the angular response of the quasi-Lambertian detector. Sampling is every 20 seconds. The central wavelength and FWHM for each filter is given in Table 1. The temperature is held at 40°C. Calibration was based on a robust estimate using the 20 nearest successful Langley plots at SGP.

The rotating shadowband spectroradiometer (RSS) [*Harrison et al.*, 1999] has a Lambertian receiver and a shadowing sequence similar to the MFRSR, however, the detector is a 512-element photodiode array that receives its energy input from the focus of a prism spectrograph. Sampling is performed once each minute. The spectral resolution between 350 and 1050 nm diminishes from 0.3 to 8 nm because of the prism dispersive element. The temperature is held at 40°C. The calibration procedure is identical to that employed for the MFRSR using the 20 nearest successful Langley plots at SGP. One of those 20 nearest successful Langley plots was obtained with data from the morning of September 29. A Langley plot performed with AATS-6 during that same morning yielded calibration constants that agreed within 0.5% with the Mauna Loa results obtained two weeks before the IOP. This suggests that during this particular morning the atmosphere over SGP was sufficiently stable to yield unbiased Langley plot results to be used in the robust estimate of the calibration constants for MFRSR and RSS.

Pennsylvania State University (PSU) deployed an early generation sunphotometer fabricated at the University of Arizona [*Shaw et al.*, 1973]. After the IOP it was discovered that the filter wheel of that instrument had slipped slightly in the drive shaft and therefore the filters would not necessarily be perfectly aligned with the optical axis. Indeed the AODs obtained from that instrument revealed a positive bias and considerable scatter when compared to the other four instruments. Therefore we have excluded the data of the PSU sunphotometer from the comparisons shown below.

Table 2a. CIMEL minus AATS-6 (15 days, 461 pts)

AATS-6	CIMEL						
λ [nm]	λ [nm]	Bias	Std	U_{95}[a]	RMS	Slope	Inter
380.1	380	0.006	0.011	0.023	0.012	0.971	0.011
450.7	*450.7*[b]	0.003	0.008	0.016	0.008	0.970	0.007
525.3	*525.3*	0.010	0.006	0.016	0.012	1.010	0.009
863.9	870	0.003	0.009	0.018	0.009	0.859	0.010
1020.7	1020	-0.001	0.006	0.012	0.006	0.940	0.002

[a] $U_{95} = \sqrt{\text{Bias}^2 + (2 \cdot \text{Std})^2}$

[b] AOD has been interpolated if wavelength is printed in Italics

Table 2b. MFRSR minus AATS-6 (11 days, 14,678 pts)

AATS-6	MFRSR						
λ [nm]	λ [nm]	Bias	Std	U_{95}	RMS	Slope	Inter
450.7	*450.7*	-0.002	0.013	0.026	0.013	0.897	0.012
525.3	*525.3*	0.000	0.011	0.022	0.011	0.905	0.009
863.9	859.9	0.002	0.012	0.024	0.012	0.745	0.015

3. Results

The instruments used in this study were located in the same general area of the ARM SGP central facility, but were spread over a distance of about 150 m. The AODs obtained with each instrument were compared with the values measured with AATS-6, since it was expected to be the most accurate with a calibration just two weeks earlier at Mauna Loa. The nearest samples in time to the AATS-6 were used to derive bias, standard deviation of the differences, U_{95} [*International Organization for Standardization*, 1995] derived from these two quantities, root-mean-squared differences, and slope and intercept of the best fit line (see Table 2). A first-order cloud filtering was achieved by comparing only with those AATS-6 AOD samples that yielded an Ångström parameter α>0.75. This resulted in as few as 461 samples to as many as 14,678 samples in the comparisons because of the different sampling strategies and days of operation. The AOD comparisons between AATS-6 and the other instruments are made for those filters whose central wavelengths match (for λ=380 nm) or are within 6-8 nm ($\lambda \geq 519$ nm) of each other. For the other wavelengths the AODs where interpolated to the AATS-6 wavelength on a log λ vs. log AOD scale.

The AODs obtained from each instrument were derived independently of one another. Although the methods to remove Rayleigh, ozone and nitrogen dioxide optical depths

Table 2c. RSS minus AATS-6 (10 days, 4508 pts)

AATS-6	RSS						
λ [nm]	λ [nm]	Bias	Std	U_{95}	RMS	Slope	Inter
380.1	*380.1*	-0.018	0.018	0.040	0.025	0.881	0.006
450.7	*450.7*	-0.009	0.012	0.026	0.015	0.893	0.007
525.3	*525.3*	-0.004	0.009	0.018	0.010	0.906	0.007
863.9	*863.9*	-0.006	0.012	0.025	0.013	0.706	0.011
1020.7	*1020.7*	-0.004	0.008	0.016	0.009	0.789	0.007

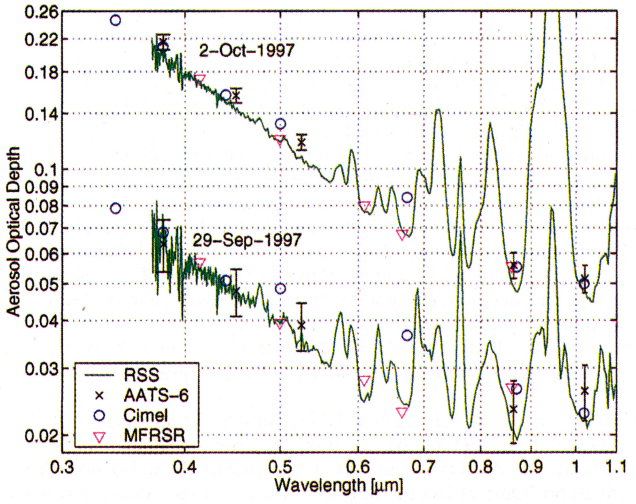

Figure 1. Average aerosol optical depth versus wavelength on 29 September 1997 (13:00-16:22 local time), a low turbidity day and 2 October 1997 (11:12-16:36 local time) a moderately turbid day. For RSS the net optical depth after subtracting Rayleigh scattering and ozone optical depths is shown. The broad peaks that remain are the result of absorption by water vapor, molecular oxygen, and collision-induced absorption by molecular oxygen pairs.

may coincide in some instances, there was no attempt at a uniform reduction to aerosol optical depth from total optical depth. Consequently, some differences based on ozone assumptions or pressure corrections and the precise form of the Rayleigh and ozone calculations may add to the differences shown in Table 2. Rayleigh optical depth has been computed according to *Bucholtz* [1995] for CIMEL and AATS-6 and according to *Hansen and Travis* [1974] for MFRSR and RSS. However Bucholtz's values are only slightly higher, 0.002 at 380 nm and 0.001 at 450 nm, and virtually identical at longer wavelengths. Differences in ozone assumptions are negligible for the wavelengths shown in Table 2, but more important for RSS and MFRSR wavelengths near the center of the ozone Chappuis band (565-615 nm). For these two instruments the ozone optical depth is computed using total column ozone values taken from the Total Ozone Monitor Sensor (TOMS) on the Earth Probe satellite and the absorption cross-sections given by *Shettle and Anderson* [1995].

The best agreement with the AATS-6 overall was with the CIMEL leading to rms differences between 0.006 and 0.012, and U_{95} between 0.012 and 0.023. Also the slopes of the best-fit lines are closest to unity when AATS-6 is regressed versus CIMEL. The Cimel AODs tend to be slightly higher, 0.003 to 0.010, than the AATS-6 values. Comparing AATS-6 and MFRSR leads to virtually no bias, but to slightly larger rms differences and U_{95} values. Similar were results obtained between the AATS-6 and the RSS with the exception of the 380-nm channel of the RSS with a bias of 0.018 and an rms difference of 0.025 optical depths. The slopes of the regression lines for MFRSR and RSS are smaller than unity at all wavelengths compared. When regressing AATS-6 against any of the three other instruments, the largest deviation of the slope from unity is always found at 863.9 nm.

Figure 1 shows temporally averaged spectral aerosol optical depth on days with low and moderate aerosol loading (September 29 and October 2, repectively). The solid line in both spectra is the RSS net optical depth after subtracting a Rayleigh scattering optical depth and an ozone optical depth. The broad peaks that remain are the result of absorption by water vapor, molecular oxygen, and collision-induced absorption by molecular oxygen pairs. As is clearly seen, filters in the other instruments are selected to avoid these bands in order to measure aerosol optical depths. The AODs from the filtered instruments agree with the RSS AODs within 0.015 at all wavelengths. The error bars on the AATS-6 data points include the uncertainty in Langley calibration, measured signal, airmass and gaseous absorption optical depths [*Russell et al.*, 1993].

Figure 2, shows a time series of AOD obtained from the four radiometers on September 29 at wavelengths near 865 nm. The maximum AOD difference is 0.015. Figure 3

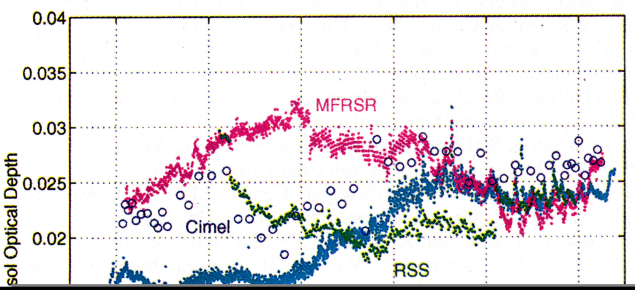

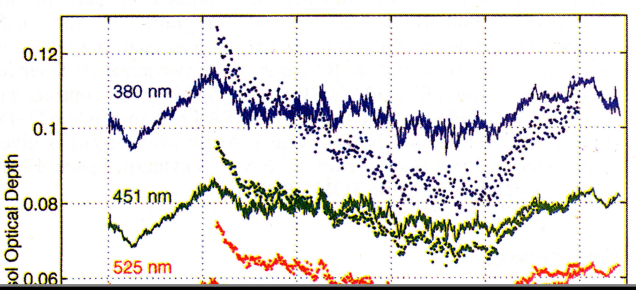

shows a time series of AOD of RSS and AATS-6 at the five AATS-6 aerosol wavelengths for September 27. Agreement throughout the day is 0.02 at 380 nm and 0.015 or better at the other wavelengths.

4. Conclusion

It should be pointed out that we have differenced the results in Table 2 with a single instrument (AATS-6) that was considered the most well-calibrated of the instruments, but which is not without error. Consequently, some of the differences can be attributed to the reference instrument. The two instruments whose calibrations are tied to Langley calibrations at Mauna Loa and which rely on measuring the direct solar beam (CIMEL and AATS-6) show the best agreement. The MFRSR and RSS, with calibrations based on the same robust technique employing 20 "on-site" Langley events, and which rely on subtracting the diffuse from the total component, agree closely with each other and agree within 0.025 (rms) with AATS-6. Excluding the RSS results at 380 nm the agreement is within 0.015 (rms).

In conclusion, we find that the four well-calibrated instruments used in this comparison can retrieve AOD in the spectral range from 380 to 1020 nm with an accuracy of at least 0.04 (U_{95}) or more typical 0.026 (if the RSS results at 380 nm are excluded), which is close to the 0.02 AOD accuracy (2 sigma) suggested as a goal by the WMO [1993]. Encouraging is the fact that these accuracies were achieved for measurements at a site typical of where these measurements are required, rather than at an ideal mountain location. In future attempts to repeat and improve on this experiment the reduction of total optical depths to aerosol optical depths should be based on identical algorithms applied to all of the data.

This experiment also showed that an intercomparison may be required to detect an instrument malfunction. We therefore conclude that in addition to meticulous care in the calibration of the instruments, periodic instrument intercomparisons are essential in order to measure AOD within the accuracies stated above.

Acknowledgments. This research was funded in part by the Atmospheric Radiation Measurement program of the U.S. Department of Energy; the Office of Energy Research; the Office of Biological and Environmental Research; the Environmental Sciences Division by grant DE-FG02-90ER61072 (SUNY), by contract no. DE-AC02-98CH10886 (BNL), and by NASA Program Code 622-44-10-10 (BAERI, SRI, and NASA Ames). Acknowledgement is given to the Ozone Processing Team at NASA Goddard Space Flight Center for making available TOMS EP data.

References

Bucholtz, A., Rayleigh-scattering calculations for the terrestrial atmosphere, *Appl. Opt., 34*, 2765-2773, 1995.

Hansen, J. E., and L. D. Travis, Light scattering in planetary atmospheres, *Space Sci. Rev., 16*, 527-610, 1974.

Harrison, L., J. Michalsky, and J. Berndt, Automated multifilter rotating shadow-band radiometer: an instrument for optical depth and radiation measurements. *Appl. Opt., 33,* 5118-5125, 1994.

Harrison, L., M. Beauharnois, J. Berndt, P. Kiedron, J. Michalsky, Q. Min: The rotating shadowband spectroradiometer (RSS) at SGP, *Geophys. Res. Lett., in press*, 1999.

International Organization for Standardization, "Guide to the Expression of Uncertainty in Measurement", ISBN 92-67-101889, 1995.

Holben, B. N., T. F. Eck, I. Slutsker, D. Tanré, J. P Buis, A. Setzer, E. Vermote, J. A. Reagan, Y. J. Kaufman, T. Nakajima, F. Lavenu, I. Jankowiak, and A. Smirnov, AERONET: a federated instrument network and data archive for aerosol characterization. *Remote Sens. Environ., 66*, 1-16, 1998.

Matsumoto, T., P. B. Russell, C. Mina, and W. Van Ark, Airborne tracking sunphotometer. *J. Atmos. Ocean. Tech., 4*, 336-339, 1987.

Russell, P. B., J. M. Livingston, E. G. Dutton, R. F. Puschel, J. A. Reagan, T. E. Defoor, M. A. Box, D. Allen, P. Pilewski, B. M. Herman, S. A. Kinne, and D. J. Hofmann, Pinatubo and Pre-Pinatubo Optical-Depth Spectra: Mauna Loa Measurements, Comparisons, Inferred Particle Size Distributions, Radiative Effects, and Relationsship to Lidar Data, *J. Geophys. Res., 98*, 22,969-22,985, 1993.

Shettle, E. P., and S. M. Anderson, New Visible and Near IR Ozone Absorption Cross-Sections for MODTRAN, *Proceedings of the 17th Annual Conference on Atmospheric Transmission Models, 8-9 June 1994.* PL-TR-95-2060 Special Reports, No 274, G. P. Anderson, R. H. Picard, and J. H. Chetwind, (Eds.), Phillips Laboratory Directorate of Geophysics, Hanscomb, AFB, MA 01731-3010, 335-350, 1995.

Schmid, B., P. R. Spyak, S. F. Biggar, C. Wehrli, J. Sekler, T. Ingold, C. Mätzler, and N. Kämpfer, Evaluation of the applicability of solar and lamp radiometric calibrations of a precision Sun photometer operating between 300 and 1025 nm, *Appl. Opt., 37*, 3923-3941, 1998.

Shaw, G. E., J. A. Reagan and B. M. Herman, Investigations of Atmospheric Extinction Using Direct Solar Radiation Measurements Made with a Multiple Wavelength Radiometer. *J. Appl. Meteorol., 12*, 374-380, 1973.

World Meteorological Organization, Report of the WMO workshop on the measurement of atmospheric optical depth and turbidity. Silver Spring, Maryland, 6-10 December 1993, Bruce Hicks (Ed.), obtainable from WMO as Technical Document No. 659 (Geneva, Switzerland), URL: www.wmo.ch, 28 pp, 1993.

B. Schmid, Bay Area Environmental Research Institute, 3430 Noriega Street, San Francisco, CA 94122. (e-mail: bschmid@mail.arc.nasa.gov)

M. Beauharnois, L. Harrison, and J. Michalsky, Atmospheric Sciences Research Center, State University of New York, Albany, 251 Fuller Road, Albany, NY 12203. (e-mail: mark, lee, or joe@asrc.cestm.albany.edu)

R. Halthore, Brookhaven National Lab, P.O. Box 5000, Upton, NY 11973. (e-mail: halthore@bnl.gov)

J. Livingston, SRI International, 333 Ravenswood Avenue, Menlo Park, CA 94025. (e-mail: jlivingston@mail.arc.nasa.gov)

P. Russell, NASA Ames Research Center, MS 245-5, Moffett Field, CA 94035-1000. (e-mail: prussell@mail.arc.nasa.gov)

B. Holben, T. Eck, and A. Smirnov, NASA Goddard Space Flight Center, Code 923, Greenbelt, MD 20771, (e-mail: brent, tom or asmirnov@spamer.gsfc.nasa.gov)

(Received April 26, 1999; revised: June 2, 1999; accepted June 4, 1999)